Journal of Experimental Zoology Part A: Ecological Genetics and Physiology

Salinity stress results in rapid cell cycle changes of tilapia (Oreochromis mossambicus) gill epithelial cells

Journal:	*Journal of Experimental Zoology Part A: Ecological Genetics and Physiology*
Manuscript ID:	draft
Wiley - Manuscript type:	Research Paper
Date Submitted by the Author:	n/a
Complete List of Authors:	Kammerer, Brittany; University of California, Davis, Animal Science Sardella, Brian; University of California, Davis, Animal Science; UC Davis Kültz, Dietmar; Univ. California, Davis, Animal Science
Keywords:	salinity stress, fish osmoregulation, chloride cell

Manuscript prepared for Journal of Experimental Zoology

4/18/2008

Salinity stress results in rapid cell cycle changes of tilapia (*Oreochromis mossambicus*) gill epithelial cells[1].

Brittany D. Kammerer[§], Brian A. Sardella[§] and Dietmar Kültz[§¶]

[§] Physiological Genomics Group, Department of Animal Science, University of California, Davis, One Shields Avenue, Davis, CA 95616, USA.

Running title: Salinity effects on tilapia gill cell cycle

Total Figures: 9

[¶] To whom correspondence should be addressed:

Physiological Genomics Group,

Department of Animal Science,

University of California, Davis

One Shields Avenue, Meyer Hall, Davis, CA 95616, USA.

Telephone: (530) 752-2991

Fax: (530) 752-0175

E-mail: dkueltz@ucdavis.edu.

[1] Supported by NSF # IOB-0542755

SUMMARY

We have developed a technique for immunocytochemistry of fish gill cells that we used to quantify tilapia *(Oreochromis mossambicus)* mitochondria-rich cells (MRCs) and other gill cells within different cell cycle phases by laser scanning cytometry (LSC). Gill cells fixed on coverslips were triple-stained with propidium iodide to distinguish G1 versus G2 phases, Ser10-phosphorylated histone H3 antibody to label mitotic cells, and Na^+/K^+ ATPase (NKA) antibody to label MRCs. These parameters were measured at 0 (control), 4, 8, 16, 24, 48, 72, and 168 h (1-week) following exposure of fresh water (FW) acclimated fish to 2/3 seawater (SW). MRCs increased mitotic activity very rapidly peaking at 8 h following SW exposure. This change in mitotic MRCs is indicative of epithelial reorganization during SW acclimation. In contrast to MRCs, the proportion of other gill epithelial cells in mitosis did not change significantly in response to SW exposure. Moreover, twice as many MRCs were in mitosis compared to other gill cells, suggesting that MRCs turn over faster than other cell types during SW acclimation. Following the mitosis peak, MRCs accumulated in G2 phase over a period of 16 h to 72 h post-SW exposure. We also observed G2 arrest with similar kinetics following SW exposure in tilapia gill cell types other than MRC. We interpret the G2 arrest that occurs after an initial wave of transient increase in MRC mitosis as a means for conserving energy for dealing with the osmotic stress imposed during the exposure of FW fish to SW.

INTRODUCTION

Tilapia *(Oreochromis mossambicus)* are a well-known invasive fish that can survive severe levels of environmental stress such as salinity (Stickney, '86; Sardella et al., 2004). This species is native to warm freshwater (FW) lakes in east Africa, but they have invaded habitats worldwide as a result of accidental release from aquaculture practices (Costa-Pierce, 2003). Because of their ability to tolerate a wide range of salinity, tilapia are a good model for investigation of osmotic stress effects and mechanisms by which teleosts adapt to such effects. Long-term acclimation to seawater (SW) in teleosts has been well-characterized and includes changes in membrane protein activity and abundance, e.g. Na^+/K^+- ATPase (NKA), as well as corresponding changes in mitochondria-rich cell (MRC) number and size (McCormick, '95). However, to date, while efforts on the short-term mechanisms of salinity acclimation such as osmotic stress sensing and signaling are being made (e.g. (Fiol et al., 2006; Tseng et al., 2007; Fiol and Kültz, 2007), short-term effects of salinity stress on the cell cycle of MRCs and other gill epithelial cells are unknown.

Changes in the cell cycle are commonly observed during hyperosmotic stress in mammalian cells (Mak and Kültz, 2004), and turnover of teleost MRCs increases when fish are transferred from FW to SW (Conte and Lin, '67; Chretien and Pisam, '86; Uchida and Kaneko, '96). Following transfer to hyperosmotic water, tilapia MRCs underwent a period of rapid proliferation, within 3 d at which time the MRCs begin a period of hypertrophy (Foskett et al., '81); however, how these changes affect the cell cycle of gill cells remains unknown.

Changes in cell cycle can be measured effectively by cytometry after staining nuclear DNA with fluorescent dyes (Darzienkiewicz et al., 2001; Mak and Kültz, 2004). Moreover, fluorescent antibodies against Ser10-phosphorylated histone H3 can be used as a reliable mitotic marker (Juan et al., 2001). The use of fluorescent probes in combination with a laser scanning cytometer allows for accurate quantification of the proportion of cells in the major cell cycle phases following exposure to an osmotic stress (Mak and Kültz, 2004). Such cell cycle analysis by laser scanning cytometry can be enhanced by using fluorescent NKA antibodies to distinguish MRCs from other epithelial cell types. In this regard, we have recently demonstrated that laser scanning cytometry can be used to detect and quantify fish gill MRCs based on their intensity of staining for NKA (Lima and Kültz, 2004; Sardella et al., 2007).

To utilize these approaches for cell cycle analysis of teleost gill epithelial cells, however, staining of gill tissue sections with fluorescent cell cycle indicator dyes was not an option because cell nuclei are cut at variable planes and analysis of DNA and histone content would be inaccurate. Here we present a method of cell cycle analysis that is based on 1) isolating and dissociating gill epithelial cells 2) adhering them to microscope coverslips, 3) staining coverslips with fluorescent cell cycle indicator dyes, then 4) analyzing stained coverslips by laser scanning cytometry. Using this approach, we quantified changes in the MRC and PVC cell cycle, and NKA concentration per MRC that occur rapidly in response to salinity stress.

METHODS

Animals

Tilapia (*Oreochromis mossambicus)* grown from FW laboratory stock, were maintained at 24- 27°C at the UC Davis Center for Aquatic Biology and Aquaculture. Fish, 10± 0.3 cm (20.1± 1.8 g), were then transferred to 38 l glass aquaria filled with FW and fitted with air stones and Fluval filters. They were maintained at 24-27°C and fed commercial trout pellets up to 2 d before sampling. After a 3 d pre-acclimation period to the glass aquaria, tilapia were exposed to 2/3 SW (23 g l^{-1}) by first draining tanks to 1/3 freshwater and refilling to full-volume with appropriately warmed ocean SW, collected from the UC Davis Bodega Bay Marine Laboratory. Fish were then allowed to acclimate and sampled at 0, 2, 4, 8, 16, 24, 72, and 168 (1-week) h. Temperature was held at 24-27°C during all exposures and water was filtered to control ammonia accumulation. Salinity was monitored using a light refractometer and water osmolality by freezing-point osmometry (µOsmette, Model 3300 Advanced Instruments, Inc).

Gill epithelial cell dissociation

Fish were sacrificed by rapid spinal transection, and gills were then perfused with ice-cold 1x Ca^{2+}-, Mg^{2+}-free phosphate buffered saline (PBS), using a Fisher Ultra-low flow peristaltic pump, which was effective for clearing gills of red blood cells. Gill epithelium was scraped from the filaments using a scalpel and mechanically disassociated into single cell suspensions. The use of a cell sieve kit (Sigma CD-1) in combination with a flat glass pestle and nylon mesh (100 µm, Small Parts Co.) (Bell et al., '92; Galvez et al., 2006) yielded cell suspensions of better integrity than a porcelain pestle or other mesh

as evaluated by phase contrast microscopy (VWR) after centrifugation of cell suspensions on to coverslips (Figure 1, see below).

Attachment of cell suspensions to coverslips and fixation

Following cell disassociation, cells were pelleted at 500g for 1 minute, counted in a haemocytometer (Hausser Scientific) and diluted to 2-3 x 10^6 cells/ml in cold PBS. Once diluted, cell suspensions (0.5 ml) were centrifuged on to poly-L-lysine (Sigma P4832) coated coverslips in 12-well microtiter plates using an Eppendorf 5804R centrifuge with a microtiterplate swing-bucket rotor (A-2-DWP, Eppendorf) at 4000 g for 5 minutes at 4°C to maximize the amount of cell adherence to coverslips. These conditions were optimized to maximize cell integrity as well as minimize cell lysis during subsequent immunocytochemistry (ICC) procedures. Following centrifugation, cells were fixed for 15 min. in 1% methanol-free formaldehyde at pH 7.4 (diluted from 10% stock solution - PolySciences, Inc. # 04018 - with PBS). Cells were then rinsed once with PBS and stored overnight in 70% ethanol at -20 °C. Appropriate cell fixation proved critical for cell integrity during ICC. Several fixation methods were tried unsuccessfully, including 100% methanol fixation and 100% ethanol fixation (Pollice et al., '92; 2000; Dmitrieva et al., 2000). These methods either led to cell damage or detachment of cells from coverslips. Para-formaldehyde (Pollice et al., '92; 2000) was tested as an alternative to formaldehyde by comparing cell integrity at 0.25%,0.5%, 1%, 3%, and 4% concentration and fixation times ranging from 15 to 120 min. Para-formaldehyde was prepared fresh by first mixing powder with PBS (pH 7.4) and then filtering the solution through 0.45 µm filter disks to decrease autoflourescence (Pollice et al., '92; Stewart and

Stewart, 2001). However, freshly prepared, ultrapure, methanol-free formaldehyde (pH 7.4, PolySciences, Inc. # 04018) was overall superior to para-formaldehyde with this procedure. For overnight storage of fixed coverslips 70% ethanol turned out better than 100% ethanol or 100% methanol, presumably because of decreased evaporation and better preservation of protein antigenicity (Juan et al., 2001; Koester and Bolton, 2001).

DNA staining and immunocytochemistry

After overnight storage in 70% ethanol, coverslips were rinsed briefly by dipping in PBS three times and incubated for 5 min. in PBS containing 0.5% Triton X-100 (4°C), adjusted to biological pH (7.4). This incubation step was necessary to make cells' nuclear envelopes permeable and thus facilitate access of DNA stain and histone H3 antibodies to their nuclear targets (Endl et al., 2001). Cell-coated coverslips were then rinsed three times for 5 min. with PBS and incubated in PBS containing 2% bovine serum albumin (PBA) for 30 min. followed by 30 min. blocking in 2% goat IgG in PBA. Primary antibody against NKA avian α-subunit developed by Douglas M. Fambrough was obtained from the Developmental Studies Hybridoma Bank instituted under the auspices of the National Institute for Child Health and Human Development (NICHD) and maintained by the University of Iowa, Department of Biological Sciences, Iowa City, IA 52242, USA. The primary NKA antibody was diluted in PBA to 1:50 concentration, while phospho-histone (H3) Ser10 mitotic primary antibody (Upstate Biotechnology, Inc. #06-570) was diluted 1:200 and fixed cells co-incubated with both antibodies for 1 h. Cell- coated coverslips were then rinsed 3 times for 5 min. in PBS in 12-well plates. Pacific-Blue labeled (Invitrogen P-10993) and anti-rabbit Alexa488-labeled (Invitrogen,

Molecular Probes #A11034) secondary antibodies were diluted to 1:100 in PBA and then 1/100th (v/v) of 100 µg/ml thawed RNAase solution was added (Sigma R-5000, for RNA hydrolysis). Coverslips were rinsed in PBS three times for 5 min. and incubated in propidium iodide (PI) solution (1:500) for 5 min. Following PI incubation, staining solution was removed and replaced with PBS. Coverslips were stored overnight in PBS at 4 ^{o}C in parafilm-sealed, 12-well plates and kept dark.

LSC analysis

Cells fixed to coverslips were analyzed the following day by laser scanning cytometry (LSC). They were first mounted and secured to microscope slides with 2 small drops of nail polish to prevent movement of coverslips on slides. We tested several different mounting media to minimize background fluorescence, including PBS, Vectashield (H-1000, company), Vectashield Hardset (H-1400, company), and Pro-Long Gold Anti-Fade (Invitrogen). PBS gave consistently the lowest background fluorescence. Thus, we mounted coverslips in PBS (10 µl), capitalizing on our ability to analyze these samples shortly following staining and knowing that long-term storage of these slides is not practical, based on previous trials and other studies (Murrell-Bussell et al., '98; Smolewski et al., 2001).

Trivariate LSC analysis was carried out using a laser scanning cytometer (Compucyte) equipped with an argon ion laser (488 nm) for Alexa488 and PI, and a UV-blue laser (400nm) for Pacific-blue. Fluorescence was recorded using violet, green, and red emission photomultiplier tubes (PMTs) of the LSC. For each coverslip, an area of identical size was scanned with a 20x fluorescence objective. Cell nuclei and NKA

fluorescence were detected and contoured with Wincyte software (v. 3.6, Compucyte) based on PI, Alexa488, and Pacific blue fluorescence. Flourescence intensities are expressed as relative fluorescent units (RFU). Micrographs and cell galleries were recorded using Wincyte software (Mak and Kültz, 2004), while cell pictures were taken using fluorescent microscopy (Olympus BX51) and digital camera (Sony MPEG MovieEX DSC-F704) still recording.

Statistics

Data analysis was carried out with Sigmastat software (v3.5), while graphs were made using Sigmaplot (9.0) or Microsoft Excel. The effects of time of salinity exposure on cell type, taking into account the interactive effect of the two variables, were analyzed by two-way ANOVA using the F-test, followed by post-hoc Tukey HSD test on values transformed by arcsine squareroot for proportions. Additionally, the effect of time of salinity exposure on UV-Blue Intensity per MRC was evaluated using one-way ANOVA followed by post-hoc Tukey HSD test. Significance was set at $p< 0.05$ for all tests and values reflect the average of six replicates, presented as the mean± standard error of the mean (S.E.). A minimum of 4000 cells per sample scan area (5 mm^2) were analyzed.

RESULTS

Co-labeling of gill cell preparations with antibody against Na^+/K^+ ATPase (NKA) and antibody against Ser10-phosphorylated histone H3 enabled us to distinguish mitochondria-rich cells (MRC), mitotic MRCs, non-MRCs, and mitotic non-MRCs by laser scanning cytometry (Figure 2). We were able to determine the proportion of each of these cell populations in G1 or G2 cell cycle phase based on propidium iodide (PI) staining. The amount of PI intensity, which is indicative of the amount of DNA in gill cell populations, was quantified using LSC (Figure 3). The cell cycle was analyzed in all gill cells present on each coverslip within a representative scan area (5 mm^2). Cells in G2 phase were distinguished from those in G1 by having on average twice as much DNA in their nuclei and consequently having twice as intense PI fluorescence (Figure 3A). The concentration of NKA per MRC was then quantified and a NKA UV-blue fluorescence threshold set below which no MRC were found. This threshold value was based on extensive verification of actual cell images using Wincyte image galleries to make sure that it accurately separated MRC from other gill epithelial cells. The threshold value determined from this analysis was 5000 relative fluorescence units (Figure 3B). Using this threshold we were able to separately analyze cell populations above and below the MRC detection threshold for their proportions of histone H3 (Ser10) positive (mitotic) cells (Figure 3C, D). Likewise, cell populations above and below the MRC detection threshold were analyzed for their proportions of G1 cells and G2 cells (Figure 3E, F). Gill cells of FW tilapia were predominantly in the G1 cell cycle phase. This was true for all cell types analyzed (Figure 4A, B); however, after 72 h of exposure to 2/3 SW, most were in G2 (Figure 4C, D).

We were interested whether the observed accumulation of cells in G2 phase after exposure to salinity stress was a transient event and how long it would prevail. Thus, we carried out an experiment in which the time course of cell cycle changes in response to salinity stress was recorded. The results of this experiment show that the increase in proportion of cells in G2 was transient with a peak at 3 d, and that pre-exposure proportions of cells in G2 phase were restored within 1 week. The kinetics of change in ratio of cells in G2 was virtually identical in MRC and other gill epithelial cells ($F= 0.133$, $p=0.716$), where the proportion of epithelial cells in G2 differed from FW-control as early as 16h (Figure 5A, B) ($p<0.05$). The magnitude of transient change in proportion of cells in G2 was large in all major gill epithelial cell types. MRCs that are in G2 phase of the cell cycle significantly increased from 0.219 ± 0.011 (21.95 ± 1.1%) prior to salinity exposure to 0.361 ± 0.043 (36.1 ± 0.43%) at 16h ($p<0.05$) and up to 0.408 ± 0.040 (40.8 ± 3.95 %) at 3 d ($F=8.382$; $p<0.001$) before dropping again after 1 week (Figure 5A). Non-MRCs that were in G2 phase of the cell cycle showed a similar trend, significantly increasing from 0.192 ± 0.016 (19.24 ± 1.62 %) prior to salinity exposure to 0.312 ± 0.031 (31.18 ± 3.11%) at 16 h ($p<0.05$) and up to 0.41 ± 0.043 (40.67 ± 4.37%) at 3 d ($F=3.855$; $p<0.001$) before dropping again after 1 week (Figure 5B). Consistent with the transient accumulation of cells in G2 phase there was a transient decrease of MRCs and other gill epithelial cell types that were in G1 phase of the cell cycle when tilapia were exposed to salinity stress, with no significant difference between cell types ($F=2.125$; $p=0.149$). MRCs that were in G1 phase of the cell cycle significantly decrease from 0.558 ± 0.012 (55.75 ± 1.27 %) prior to salinity exposure to 0.392 ± 0.042 (39.16 ± 4.248 %) at 16 h ($p< 0.01$) and up to 0.36 ± 0.038 (35.80 ± 3.79 %) at 3 d ($F=7.648$;

p<0.001) before rising again after 1 week (Figure 6A). Non-MRC that were in G1 phase of the cell cycle also significantly decreased from 0.615 ± 0.024 (61.5 ± 2.35%) prior to salinity exposure to 0.44 ± 0.034 (44.4 ± 3.43 %) at 16 h to as much as 0.368 ± 0.045 (36.8 ± 4.55 %) at 3 d (F=7.648; p<0.001) before rising again after 1 week (Figure 6B).

SW exposure resulted in a rapid and significant increase in mitotic MRCs that was detected and quantified by LSC analysis of phospho-histone (H3) Ser10 antibody staining and not observed in the other gill epithelial cells (Figure 7) (F=44.431, p<0.001). The proportion of mitotic MRCs increased significantly from 0.048 ± 0.008 (4.763 ± 0.77%) at time zero to 0.088 ± 0.094 (8.804 ± 0.94 %) after 8 h of SW exposure (p<0.05). Following the rapid initial spike in MRC mitosis at 8 h, mitotic MRC decreased at 16 – 72 h below control levels (p=0.001) (Figure 7A), correlating well with the onset of the change in proportion of cells in G2 that peaks at 72 h. Moreover, after 1 week of salinity acclimation the proportion of mitotic MRCs was similar to those of the control (Figure 7A), which was again consistent with the change in proportion of cells in G2 at that time.

The proportion of non-MRCs in mitosis did not increase significantly after SW exposure indicating that this behavior represented a unique property of MRCs (Figure 7B) (F=4.284; p>0.05). However, the proportion of mitotic non-MRCs showed a trend where at 16 and 72 h, levels were below that of FW (t=0) (Figure 7B), similar to what was observed for MRCs and again consistent with the change in proportion of cells in G2 phase of non-MRCs peaking at 72 h. Like for MRCs, after 1 week of salinity acclimation the proportion of mitotic non-MRCs (0.03 ± 0.004) was similar to FW controls (0.03 ±

0.005) (Figure 7B). Interestingly, the proportion of MRC's undergoing mitosis was about twice as high as that of mitotic non-MRC's at any given time point ($p < 0.05$) (Figure 8).

NKA concentration within MRC as evaluated by assessment of NKA α5-subunit abundance in individual MRC's showed an increase in response to salinity acclimation that levels off at 3 d and remained constant for at least 1 week ($F=6.585$; $p<0.001$) (Figure 9). Although the observed increase was moderate (about two-fold), it was gradual over time and significant as early as 8 h ($p<0.05$) after salinity acclimation indicating that NKA levels in MRCs increase rapidly in response to salinity challenge.

DISCUSSION

We have established a novel method for quantifying the proportion of mitochondria-rich cells (MRCs) and other gill epithelial cells within the various phases of the cell cycle using laser scanning cytometry (LSC). Using fluorescent nuclear DNA staining, we distinguished between cells in G1 versus G2, and quantified the number of mitotic cells using Ser10-phosphorylated histone H3 staining. These techniques were previously established in other studies using mouse or human cell models (Darzienkiewicz et al., 2001; Juan et al., 2001; Mak and Kültz, 2004), but we have used them for the first time to assess isolated branchial cells from a whole fish following salinity challenge. Anti-NKA antibodies have been used to identify and measure MRC size, abundance, and NKA per MRC in teleost fish species using LSC (Lin et al., 2003; Lima and Kültz, 2004; Allen, 2005; Sardella et al., 2007) in addition to other forms of microscopy (Hwang '87; Kültz et al., '95; Hiroi et al., 2005) and we were able to quantify the NKA concentration within individual MRCs in an entire population of branchial cells.

Salinity challenge resulted in a large increase in the proportion of mitotic MRCs, which peaked 8 h following the transfer (Figure 7a). The immediate increase in mitosis is consistent with the hyperplasia that was previously observed by Foskett et al. ('81) in tilapia following transfer to SW. The timing of the mitotic increase in the current study differs slightly from what was observed previously, which is likely due to methodological differences with respect to acclimation and analytical techniques. Following the peak at 8 h, the proportion of mitotic MRCs returned to near pre-exposure levels (Figure 7a). The cellular changes observed in our study as well as those observed by Foskett et al., ('81) coincide with the period identified as the "crisis period" for tilapia with respect to salinity acclimation (Hwang et al., '89); during this period, tilapia must survive a near-lethal dehydration. Our data now indicate that during this period there was substantial cellular rearrangement of the branchial epithelium.

While a rapid increase in hyperplasia alone is a plausible explanation for the dramatic increase in mitotic MRC proportions up to 8 h, this result can also be explained by an arrest of the tilapia MR cell cycle at an intra-mitotic checkpoint. Hyperosmolality has been shown to induce growth arrest in mammalian cells of the kidney, an analogous environment to that of the fish gill exposed to SW (Kültz et al., '98; Mak and Kültz, 2004). Likewise, it has been shown in yeast, that the cell cycle may be accelerated initially, then halted in mitosis in response to osmotic stress as a result of mitotic checkpoint control (Humphrey and Enoch, '98).

Coincident with the recovery of mitotic rate, we also observed a shift in the proportion of MRCs within various stages of the cell cycle, with a clear shift in the majority from G1 to G2 (Figure 5a & 6a). The large increase in number of MRCs in G2

phase may indicate an arrest at the G2/M checkpoint due to hyperosmotic stress; this has previously been observed in mammalian models (Dmitrieva et al., 2002; Mak and Kültz, 2004). The arrest of MRCs at the G2/M checkpoint correlates well with the hypertrophy of MRCs and synthesis of NKA that has been observed in SW-exposed tilapia previously (Hwang, '87; Hwang et al., '89; Kültz et al., '95). In summary, our data support previously characterized proliferation in MRCs following salinity transfer by indicating an increase in MRC mitosis. The observed change in G1/G2 ratio coincides with the period of hypertrophy that has been documented for this species. The causes for this arrest are unclear, however it may be that cellular energy is more efficiently devoted to the development of ionoregulatory mechanisms under these conditions and that energy priorities for other cellular processes such as replication are minimized.

We also observed an increase in NKA concentration within MRCs that coincided with the shift in the G1/G2 ratio and the previously documented period of hypertrophy. NKA levels per MRC increase as early as 8 h (Figure 9), and followed the recovery of mitotic cell rate (Figures 7a). It has previously been documented that MRC hypertrophy results from the synthesis of new membrane and NKA within the extensive basolateral reticulum (Dang et al., 2000). In our study NKA concentration within MRC were significantly elevated as early as 8 h following transfer, and continued to increase until 72 h, where they remain constant up to 1-week (Figure 9). These results confirm the trend seen in previous LSC studies where a larger MRC containing more NKA per unit area was seen in tilapia after 2 weeks of salinity acclimation (Sardella et al., 2007). Further, a similar trend was seen in killifish, a comparable euryhaline species, where a transient increase in NKA concentration within MRC correlated well with an increase in MRC size

up to 1-week of full-strength salinity acclimation (Lima and Kültz, 2004). Previous longer-term SW acclimation studies in tilapia indicated that an increase in MRC size, but not number, correlated with the adaptation of the gill epithelium from FW to SW in tilapia (Cioni et al., '91; Kültz et al., '95; Van Der Heijden et al., '97).

Within the non-MRC gill cells, the majority were in G1 phase of the cell cycle in FW, while upon SW exposure, their proportions shifted transiently to having most cells in G2 phase of the cell cycle as early as 16 h (Figure 5). This behavior is likely representative of pavement cells (PVC) because PVC are the most abundant cell type (Kültz et al., '95; Wilson et al., 2000) present in tilapia gill epithelium (Cioni et al., '91). Our results are consistent with those seen previously in mammalian kidney cells that increase the proportion of cells in G2 phase of the cell cycle in response to hyperosmotic stress (Mak and Kültz, 2004), as previously discussed for MRC. PVC changed the proportion of cells in G2 phase, indicative of G2/M checkpoint arrest, with similar kinetics to MRC (Figure 5).

PVC have been shown to be the location of Na^+/H^+ exchange in numerous FW teleost fish (Goss et al., '92), and V-Type H^+ ATPase and ENaC-like protein or Na^+/H^+ exchanger-like immunity have been localized to PVC in tilapia gills. Exchange of Na^+ and proton(s) are thought to contribute mostly to apical Na^+ uptake in PVCs during FW osmoregulation (Lin et al., 2003), while NKA is the dominant mechanistic protein responsible for Na^+ fluxes in SW ion exchange (Karnaky, '86). Thus, changes in PVC cell cycle in response to osmotic stress as reported in our study are consistent with functional rearrangements of PVCs upon exposure of fish to SW. Moreover, previous

studies showed that in killifish PVCs rearrange in response to SW exposure by uncovering SW MRC in the epithelium as early as 14 h (Laurent et al., 2006).

PVC arrest in G2 phase of the cell cycle corresponded well with the decreasing trend in mitotic PVCs at 16 and 72 h (Figures 5 & 7b), indicative of energy in the epithelium being directed away from proliferation of PVCs. Our results confirm those observed in similar euryhaline species (e.g. killifish or guppy) where no change in mitotic events occurred upon SW acclimation in PVC (Chretien and Pisam, '86; Laurent et al., 2006). Thus, while PVC show cell cycle arrest in response to SW in tilapia, they do not appear to increase proliferation as the epithelium adjusts; again, this observation suggests a reduced role of PVCs for SW osmoregulation and that cellular energy is redirected toward adaption and away from proliferative processes (Kültz et al., '98).

Interestingly, the percentage of PVC in mitosis is about half that of mitotic MRC at critical SW exposures, up to 1-week (Figure 8), suggesting that MRC turn over faster than PVC in response to salinity stress. This result is comparable with observations made with transmission electron microscopy in the same species, where an increased frequency of apoptotic cells indicated that the turnover rate of MRC increased in SW (Wendelaar Bonga and Van Der Meij, '89).

In summary, we conclude that a rapid and transient increase in mitosis contributes to the reorganization of MRCs during SW acclimation of tilapia. Taken together, our results also suggest that tilapia conserve energy during the acclimatory period after exposure to SW by induction of growth arrest in G2 phase. In addition, our data are consistent with an increased role of MRCs and a decreased role of PVCs in SW osmoregulation.

ACKNOWLEDGEMENTS

This project was supported by grant number IOB-0542755 from the National Science Foundation (NSF). We'd like to thank Dr. Sally Mak for her help and expert advice during the optimization of immunocytochemistry methods. We'd also like to thank Anika Liljenwall for her help with part of ICC optimization and fish care during this experiment. We'd also like to thank Dr. Thomas Famula and Jerome Braun for advice with statistical analysis during the writing of this manuscript, as well as the UC Davis Center for Aquatic Biology and Aquaculture staff for their help with the care and maintenance of fish prior to these experiments.

Abbreviations:

DNA deoxyribonucleic acid

FW freshwater

LSC laser scanning cytometry

MRC mitochondria-rich cell

MR mitochondria-rich

NKA Na^+/K^+ ATPase

PI propidium iodide

RFU Relative Flourescent Units

SW seawater

UV ultraviolet

REFERENCES

Allen PJ. 2005. Seawater adaptation in juvenile green sturgeon, *Acipenser medirostris*: The ontogeny of salinity tolerance and effects on juvenile green sturgeon chloride cells and tissue Na^+/K^+-ATPase activity, content and location. Dissertation Thesis:129-161.

Bell JG, Sargent JR, Raynard RS. 1992. Effects of increasing dietary linoleic acid on phospholipid fatty acid composition and eicosanoid production in leukocytes and gill cells of Atlantic salmon (*Salmo salar*). Prostaglandins Leukotrienes and Essential Fatty Acids 45(3):197-206.

Chretien M, Pisam M. 1986. Cell renewal and differentiation in the gill epithelium of fresh-water-adapted or salt-water-adapted euryhaline fish as revealed by [H-3] thymidine autoradiography. Biology of the Cell 56(2):137-150.

Cioni C, Merich DD, Cataldi E, Cataudella S. 1991. Fine structure of chloride cells in freshwater- and seawater-adapted *Oreochromis niloticus* (Linnaeus) and *Oreochromis mossambicus* (Peters). Journal of Fish Biology 29:197-209.

Conte FP, Lin DHY. 1967. Kinetics of cellular morphogenesis in gill epithelium during sea water adaptation of *Oncorhynchus* (Walbaum). Comparative Biochemistry and Physiology 23:945-957.

Costa-Pierce BA. 2003. Rapid evolution of an established feral tilapia (*Oreochromis spp*.): the need to incorporate invasion science into regulatory structures. Biological Invasions 5:71-84.

Dang Z, Balm PH, Flik G, Wendelaar Bonga SE, Lock RAC. 2000. Cortisol increases Na^+/K^+ ATPase density in plasma membranes of gill chloride cells in the freshwater tilapia *Oreochromis Mossambicus*. Journal Experimental Biology 203:2349-2355.

Darzienkiewicz Z, Smolewski P, Bedner E. 2001. Use of flow and laser scanning cytometry to study mechanisms regulating cell cycle and controlling cell death. Clinical Lab Medicine 21(4):857-873.

Dmitrieva N, Bulavin D, Fornace A, Jr, Burg M. 2002. Rapid activation of G2/M checkpoint after hypertonic stress in renal inner medullary epithelial (IME) cells

is protective and requires p38 kinase. Proceedings of the National Academy of Sciences (USA) 99(1):184-189.

Dmitrieva N, Kültz D, Michea L, Ferraris J, Burg M. 2000. Protection of renal inner medullary epithelial cells from apoptosis by hypertonic stress induced p53 activation. Journal of Biological Chemistry 275(24):18243-18247.

Endl E, Hollmann C, Gerdes J. 2001. Antibodies against the Ki-67 protein: assessment of the growth fraction and tools for cell cycle analysis. Methods in Cell Biology 63:399-418.

Fiol D, Chan SY, Kültz D. 2006. Regulation of osmotic stress transcription factor-1 (Ostf1) in tilapia (*Oreochromis mossambicus*) gill epithelium during salinity stress. Journal of Experimental Biology 209:3257-3265.

Fiol D, Kültz D. 2007. Osmotic stress sensing and signaling in fishes. FEBS Journal 274(22):5790-5798.

Foskett JK, Logsdon CD, Turner T, Machen TE, Bern HA. 1981. Differentiation of the chloride extrusion mechanism during seawater adaptation of a teleost fish, the cichlid *Sarotherodon Mossambicus*. Journal Experimental Biology 93:209-224.

Galvez F, Wong D, Wood CM. 2006. Cadmium and calcium uptake in isolated mitochondria-rich cell populations from the gills of the freshwater rainbow trout. American Journal of Physiology- Regulatory, Integrative and Comparative Physiology 291:R170-R176.

Goss GG, Perry SF, Wood CM, Laurent P. 1992. Mechanisms of ion and acid-base regulation at the gills of freshwater fish. Journal of Experimental Zoology 263:143-159.

Hiroi J, McCormick S, R O-K, Kaneko T. 2005. Functional classification of mitochondria-rich cells in euryhaline Mozambique tilapia (*Oreochromis mossambicus*) embryos, by means of triple immunoflourescence staining for Na^+/K^+ ATPase, $Na^+/K^+/2Cl^-$ cotransporter and CFTR anion channel. Journal of Experimental Biology 208(Pt 11):2023-2036.

Humphrey T, Enoch T. 1998. Sum1, a highly conserved WD-repeat protein, suppresses S-M checkpoint mutants and inhibits the osmotic stress cell cycle response in fission yeast. Genetics 148:1731-1742.

Hwang P, Sun CM, Wu SM. 1989. Changes of plasma osmolarity, chloride concentration and gill Na-K-ATPase activity in tilapia (*O. mossambicus*) during seawater acclimation. Marine Biology 100(295-299).

Hwang PP. 1987. Tolerance and ultrastructural responses of branchial chloride cells to salinity changes in the euryhaline teleost *Oreochromis mossambicus*. Marine Biology 94:643-649.

Juan G, Traganos F, Darzienkiewicz Z. 2001. Methods to identify mitotic cells by flow cytometry. Methods in Cell Biology 63:343-354.

Karnaky KJ. 1986. Structure and function of the chloride cell of *Fundulus heteroclitus* and Other Teleosts. American Zoology 26:209-224.

Koester SK, Bolton WE. 2001. Strategies for cell permeabilization and fixation in detecting surface and intracellular antigens. Methods in Cell Biology 63:253-268.

Kültz D, Jürss K, Jonas L. 1995. Cellular and epithelial adjustments to altered salinity in the gill and opercular epithelium of a cichlid fish (*Oreochromis mossambicus*). Cell Tissue Research 279:65-73.

Kültz D, Madhany S, Burg MB. 1998. Hyperosmolality causes growth arrest of murine kidney cells- induction of GADD45 and GADD153 by osmosensing via stress-activated protein kinase. Journal of Biological Chemistry 273(22):13645-13651.

Laurent P, Chevalier C, Wood C. 2006. Appearance of cuboidal cells in relation to salinity in gills of *Fundulus heteroclitus,* a species exhibiting branchial Na^+ but not Cl^- uptake in FW. Cell and Tissue Research 325(3):481-492.

Lima RN, Kültz D. 2004. Laser scanning cytometry and tissue microarray analysis of salinity effects on killifish chloride cells. Journal of Experimental Biology 207:1729-1739.

Lin Y, Chen C, Lee T. 2003. The expression of gill Na^+/K^+ATPase in milkfish, *Chanos chanos*, acclimated to seawater, brackish water and fresh water. Comparative Biochemistry and Physiology Part A Integrated Physiology 135(3):489-497.

Mak S, Kültz D. 2004. Gadd45 proteins induce G_2/M arrest and modulate apoptosis in kidney cells exposed to hyperosmotic stress. Journal of Biological Chemistry 279(37):39075-39084.

McCormick S. 1995. Hormonal control of gill Na^+/K^+ATPase and chloride cell function. cellular and molecular approaches to fish ionic regulation 14:285-315.

Murrell-Bussell S, Nguyen D, Schober WD, Scott J, Simpson JL, Elias S, Bischoff FZ, Lewis DE. 1998. Optimized fixation and storage conditions for FISH analysis of single-cell suspensions. The Journal of Histochemistry and Cytochemistry 46(8):971-973.

Pollice AA, McCoy JP, Jr., Shackney SE, Smith CA, Agarwal J, Burholt DR, Janocko LE, Hornicek FJ, Singh SG, Hartsock RJ. 1992. Sequntial paraformaldehyde and methanol fixation for simultaneous flow cytometric analysis of DNA, cell surface proteins, and intracellular proteins. Cytometry 13:432-444.

Pollice AA, Smith CA, Brown K, Farkas DL, Silverman JF, Shackney SE. 2000. Multiparameter analysis of human epithelial tumor cell lines by laser scanning cytometry. Cytometry (Communication in Clinical Cytometry) 42:347-356.

Sardella BA, Kültz D, Cech JJJ, Brauner CJ. 2007. The effects of temperature on chloride cell characteristics in Mozambique tilapia (*Oreochromis mossambicus*) assessed using tissue microarray analysis. Journal of Comparative Physiology. J Comp Physiology B in press.

Sardella BA, Matey V, Cooper JC, Gonzalez RJ, Brauner CJ. 2004. Physiological, biochemical and morphological indicators of osmoregulatory stress in 'California' Mozambique tilapia (*Oreochromis mossambicus* x *O. urolepis hornorum*) exposed to hypersaline water. Journal of Experimental Biology 207:1399-1413.

Smolewski P, Bedner E, Du L, Hsieh T-C, Wu JM, Phelps DJ, Darzienkiewicz Z. 2001. Detection of caspases activation by fluorochrome-labeled inhibitors: multiparameter analysis by laser scanning cytometry. Cytometry 44:73-82.

Stewart CC, Stewart SJ. 2001. Cell preparation for the identification of leukocytes. Methods in Cell Biology 63:217-251.

Stickney RR. 1986. Tilapia tolerance of saline waters - a review. Progressive Fish-Culturist 48(3):161-167.

Tseng Y-C, Huang C-J, Chang JC-H, Teng W-Y, Baba O, Fann M-J, Hwang P. 2007. Glycogen phosphorylase in glycogen-rich cells is involved in the energy supply

for ion regulation in fish gill epithelia. Comparative and Evolutionary Physiology 293:R482-R491.

Uchida K, Kaneko T. 1996. Enhanced chloride cell turnover in the gills of chum salmon fry in seawater. Zoological Science 13(5):655-660.

Van Der Heijden AJH, Verbost PM, Eygensteyn J, Li J, Wendelaar Bonga SE, Flik G. 1997. Mitochondrial-rich cells in gills of the tilapia (*Oreochromis Mossambicus*) adapted to freshwater or seawater: Quantification by Confocal Laser Scanning Microscopy. Journal Experimental Biology 200:55-64.

Wendelaar Bonga SE, Van Der Meij JCA. 1989. Degeneration and death, by apoptosis and necrosis, of the pavement and chloride cells in the gills of the teleost *Oreochromis mossambicus*. Cell Tissue Research 255:235-243.

Wilson JM, Laurent P, Tufts BL, Benos DJ, Donowitz M, Vogl AW, Randall DJ. 2000. NaCl uptake by the branchial epithelium in freshwater teleost fish: an immunological approach to ion-transport protein localization. Journal Experimental Biology 203:2279-2296.

FIGURE LEGENDS

Figure 1 Gill cell preparation for immunocytochemistry and LSC analysis. Cells were isolated from tilapia gill epithelium first by red blood cell perfusion, followed by mechanical disassociation and scraping cells from filaments. Cells were counted and resuspended, adhered to coverslips by centrifugation, fixed, and stained before LSC analysis.

Figure 2 Images of cell types analyzed by LSC during coverslip analysis. A) A relatively rare mitotic MRC, triple stained with NKA primary (1^o) and Pacific blue-labeled secondary (2^o) antibodies (blue), phospho-histone H3 (Ser10) 1^o and Alexa488-labeled 2^o antibodies (green), and PI (red) for DNA content. B) Gill MRCs are double stained with NKA 1^o and Pacific blue-labeled 2^o antibodies and PI (red) to measure DNA content. C) Mitotic cells are double stained with phospho-histone H3 (Ser10) 1^o and Alexa488-labeled 2^o antibodies (green) and PI (red). D) Other gill cells are stained with PI (red) alone.

Figure 3 Laser scanning cytometry of cell cycle analysis of tilapia gill cells exposed to seawater. Cells isolated from tilapia gills were analyzed by LSC for DNA content by propidium iodide (PI) intensity in NKA-labeled MRCs (blue) and Alexa488-labeled histone H3 (Ser10)-positive (mitotic) cells (green). A) Cytogram of amount of DNA in gill cells in different cell cycle stages, based on PI intensity B) Scattergram defining NKA-positive MRCs as cells with a UV blue peripheral integral (=blue cell contour

identified with Wincyte software) exceeding 5000 RFU. C, D) Scattergrams defining Alexa488-labelled histone H3 (Ser10) positive (mitotic) cells in non-MR gill cells (C) and MRCs (D) as cells with a green integral (=green nuclear contour surrounding the PI-defined nuclear DNA) greater than 10,000 RFU. E, F) Cytogram separating number of cells in different stages of the cell cycle in non-MRCs (E) and MRCs (F).

Figure 4 Seawater challenge results in a change in tilapia gill cells from G1 to G2 stage of the cell cycle. LSC cytograms show the number of cells in each phase of the cell cycle based on PI fluorescence intensity (identified as long red integral). G1 phase of the cell cycle is labeled brown, while G2 and S are green and pink, respectively, in each panel. FW-acclimated gill cells (t=0 hr) are mostly in G1 phase of the cell cycle in both A) non-MR gill cells and B) MRCs, while the majority of SW-acclimated gill cells: C) non-MRCs and D) MRCs are in G2 phase of the cell cycle at 72 h.

Figure 5 G2 cell cycle phase counts change in tilapia gill cells exposed to SW. Scatter plots represent the change in DNA content (measured by PI intensity) of cells in G2 stage of cell cycle. A) MRCs increase proportion of cells in G2 stage of the cell cycle at 16 h and up to 72 h SW exposure. B) Non- MRCs over time show the same trend as MRCs in G2 phase of cell cycle. Letters indicate significant differences between means (n=6).

Figure 6 G1 cell cycle stage counts change in tilapia gill cells exposed to SW. Scatter plots represent the change in PI intensity (red) indicative of DNA count. A) MRCs in G1

phase of cell cycle. B) Mean proportion of non-MRCs have the same trend as PI-stained MRCs. Letters indicate significant differences between means (n=6).

Figure 7 Seawater challenge rapidly changes mitotic cell counts in tilapia gill cells. Scatter plots represent the change in green peripheral integral (anti-phospho Histone (H3) Alexa488-labeled mitotic cells) identified by LSC. A) Proportion of MRC (blue) increase at 8 h SW exposure. B) Mean proportion of non-MRC show a trend similar to MRC, but with no difference between SW and FW controls. Letters indicate significant differences between means (n=6).

Figure 8 Salinity induces greater mitotic cell turnover in MRC than non- MRCs in tilapia gills. Comparison of mean proportion of different gill cell types in mitosis at 0, 8, and 168 h SW exposure (n=6). An astericks (*) depicts significant difference between cell types.

Figure 9 Mitochondria-rich cell NKA concentrations per MRC increase with SW exposure in tilapia gill cells. UV-Blue Peripheral Integral (blue cell contour surrounding nuclei) quantified by LSC to detect levels of Pacific blue-labeled 2^{o} antibody staining for NKA 1^{o} antibodies. Letters indicate significance between means (n=6).

Figure 1

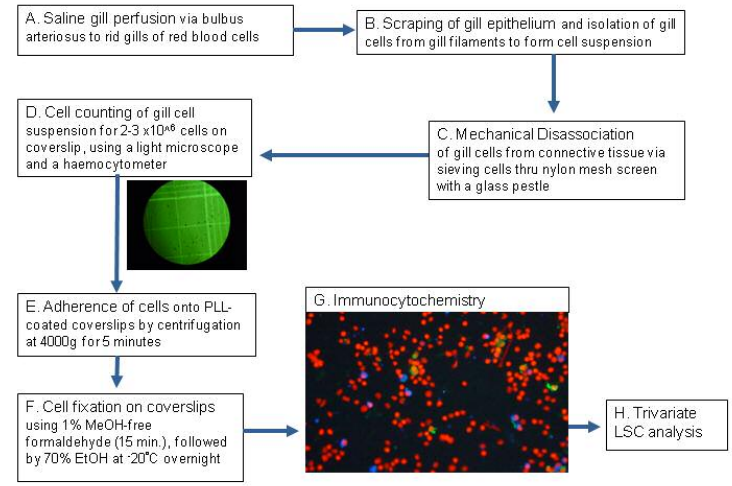

Gill cell preparation for immunocytochemistry and LSC analysis. Cells were isolated from tilapia gill epithelium first by red blood cell perfusion, followed by mechanical disassociation and scraping cells from filaments. Cells were counted and resuspended, adhered to coverslips by centrifugation, fixed, and stained before LSC analysis.
254x190mm (96 x 96 DPI)

Figure 2

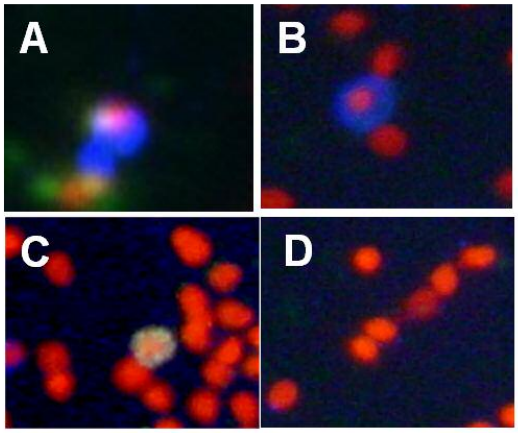

Images of cell types analyzed by LSC during coverslip analysis. A) A relatively rare mitotic MRC, triple stained with NKA primary (1o) and Pacific blue-labeled secondary (2o) antibodies (blue), phospho-histone H3 (Ser10) 1o and Alexa488-labeled 2o antibodies (green), and PI (red) for DNA content. B) Gill MRCs are double stained with NKA 1o and Pacific blue-labeled 2o antibodies and PI (red) to measure DNA content. C) Mitotic cells are double stained with phospho-histone H3 (Ser10) 1o and Alexa488-labeled 2o antibodies (green) and PI (red). D) Other gill cells are stained with PI (red) alone.
254x190mm (96 x 96 DPI)

Figure 3

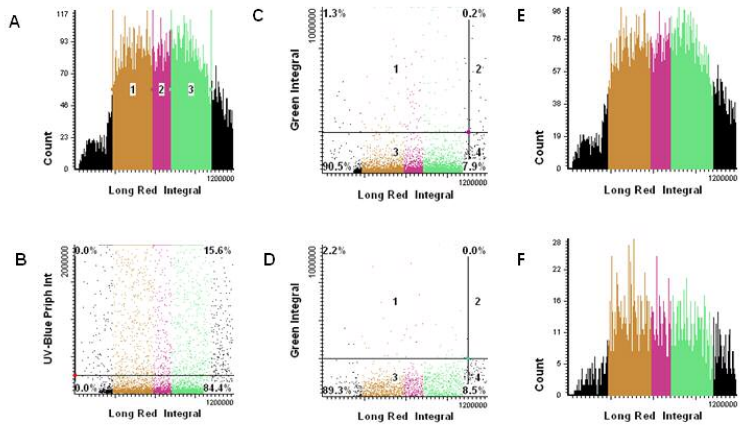

Laser scanning cytometry of cell cycle analysis of tilapia gill cells exposed to seawater. Cells isolated from tilapia gills were analyzed by LSC for DNA content by propidium iodide (PI) intensity in NKA-labeled MRCs (blue) and Alexa488-labeled histone H3 (Ser10)-positive (mitotic) cells (green). A) Cytogram of amount of DNA in gill cells in different cell cycle stages, based on PI intensity B) Scattergram defining NKA-positive MRCs as cells with a UV blue peripheral integral (=blue cell contour identified with Wincyte software) exceeding 5000 RFU. C, D) Scattergrams defining Alexa488-labelled histone H3 (Ser10) positive (mitotic) cells in non-MR gill cells (C) and MRCs (D) as cells with a green integral (=green nuclear contour surrounding the PI-defined nuclear DNA) greater than 10,000 RFU. E, F) Cytogram separating number of cells in different stages of the cell cycle in non-MRCs (E) and MRCs (F).
254x190mm (96 x 96 DPI)

Figure 4

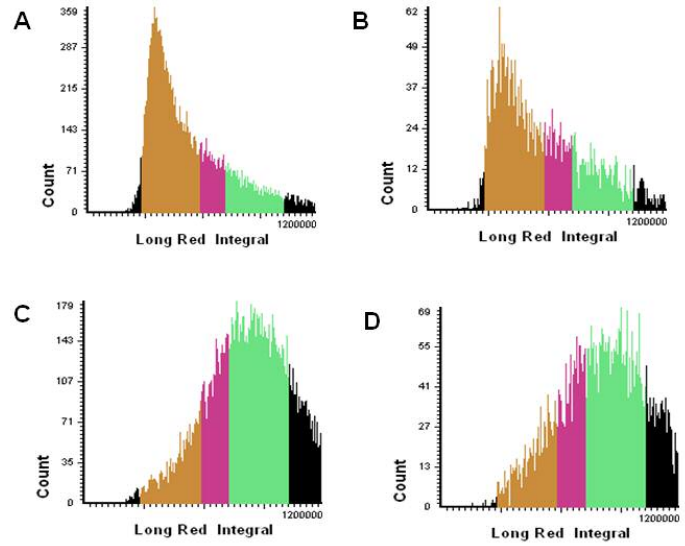

Seawater challenge results in a change in tilapia gill cells from G1 to G2 stage of the cell cycle. LSC cytograms show the number of cells in each phase of the cell cycle based on PI fluorescence intensity (identified as long red integral). G1 phase of the cell cycle is labeled brown, while G2 and S are green and pink, respectively, in each panel. FW-acclimated gill cells (t=0 hr) are mostly in G1 phase of the cell cycle in both A) non- MR gill cells and B) MRCs, while the majority of SW-acclimated gill cells: C) non-MRCs and D) MRCs are in G2 phase of the cell cycle at 72 h.

254x190mm (96 x 96 DPI)

Figure 5

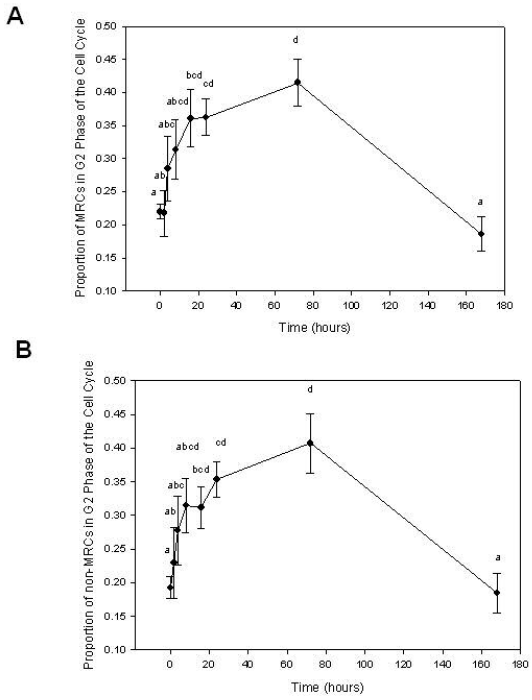

G2 cell cycle phase counts change in tilapia gill cells exposed to SW. Scatter plots represent the change in DNA content (measured by PI intensity) of cells in G2 stage of cell cycle. A) MRCs increase proportion of cells in G2 stage of the cell cycle at 16 h and up to 72 h SW exposure. B) Non- MRCs over time show the same trend as MRCs in G2 phase of cell cycle. Letters indicate significant differences between means (n=6).

254x190mm (96 x 96 DPI)

Figure 6

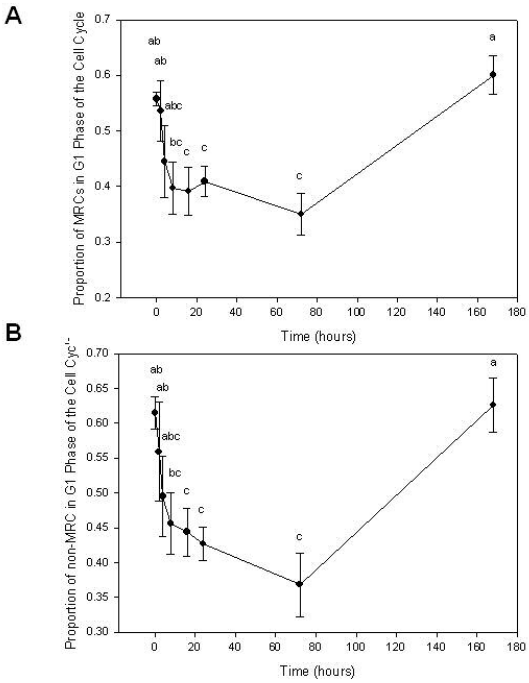

G1 cell cycle stage counts change in tilapia gill cells exposed to SW. Scatter plots represent the change in PI intensity (red) indicative of DNA count. A) MRCs in G1 phase of cell cycle. B) Mean proportion of non-MRCs have the same trend as PI-stained MRCs. Letters indicate significant differences between means (n=6).

254x190mm (96 x 96 DPI)

Figure 7

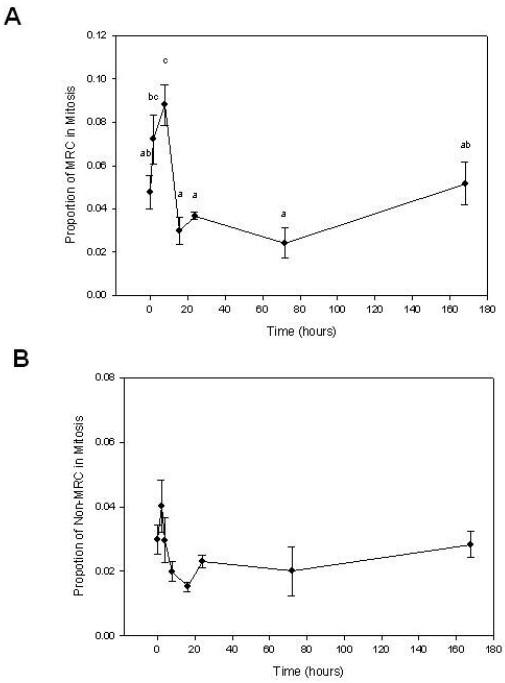

Seawater challenge rapidly changes mitotic cell counts in tilapia gill cells. Scatter plots represent the change in green peripheral integral (anti-phospho Histone (H3) Alexa488-labeled mitotic cells) identified by LSC. A) Proportion of MRC (blue) increase at 8 h SW exposure. B) Mean proportion of non-MRC show a trend similar to MRC, but with no difference between SW and FW controls. Letters indicate significant differences between means (n=6).

254x190mm (96 x 96 DPI)

Figure 8

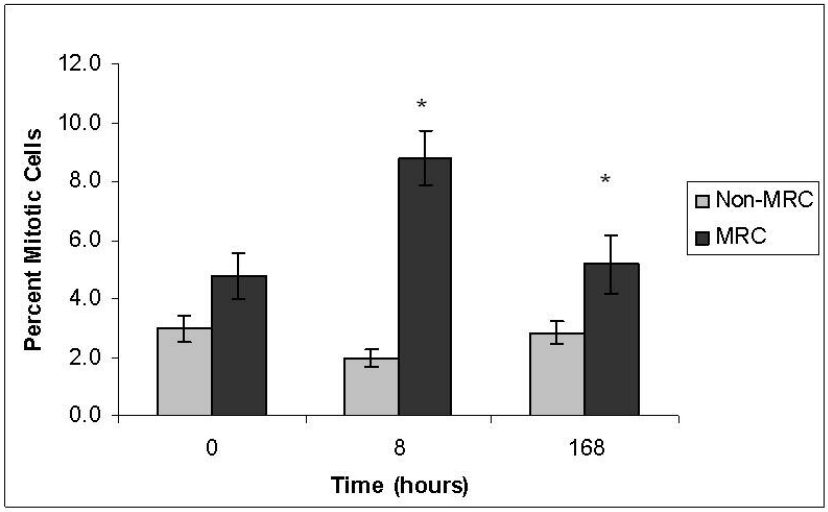

Salinity induces greater mitotic cell turnover in MRC than non- MRCs in tilapia gills. Comparison of mean proportion of different gill cell types in mitosis at 0, 8, and 168 h SW exposure (n=6). An astericks (*) depicts significant difference between cell types.
254x190mm (96 x 96 DPI)

Figure 9

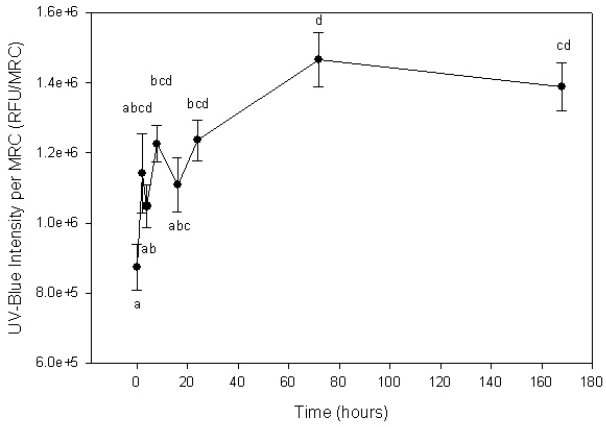

Mitochondria-rich cell NKA concentrations per MRC increase with SW exposure in tilapia gill cells. UV-Blue Peripheral Integral (blue cell contour surrounding nuclei) quantified by LSC to detect levels of Pacific blue-labeled 2o antibody staining for NKA 1o antibodies. Letters indicate significance between means (n=6).

254x190mm (96 x 96 DPI)